You may access the final editorial version published at:

https://doi.org/10.1016/j.phrs.2019.01.004

Original Research Article

Pharmacogenetics of myotonic hNav1.4 sodium channel variants situated near the fast inactivation gate

Alessandro Farinato[a], Concetta Altamura[h], Paola Imbrici[a], Lorenzo Maggi[b], Pia Bernasconi[b], Renato Mantegazza[b], Livia Pasquali[c], Gabriele Siciliano[c], Mauro Lo Monaco[d,e], Christophe Vial[f], Damien Sternberg[g], Maria Rosaria Carratù[h], Diana Conte[a], Jean-François Desaphy[h,*]

[a]Dept of Pharmacy & Drug Sciences, University of Bari Aldo Moro, Italy.

[b]Neurology IV -Neuroimmunology and Neuromuscular Diseases Unit, Fondazione IRCCS Istituto Neurologico Carlo Besta, Milan, Italy.

[c]Department of Clinical and Experimental Medicine, Section of Neurology, University of Pisa, Pisa, Italy.

[d]Institute of Neurology, Fondazione Policlinico Gemelli, IRCCS, Rome, Italy.

[e]MiA Association ("Miotonici in Associazione"),

[f]Neuromuscular Reference Center, Hospices Civils de Lyon, Bron, France.

[g]National Reference Center for Muscle Channelopathies, Groupe Hospitalier Pitié Salpetrière, Assistance Publique Hôpitaux de Paris, Paris, France.

[h]Dept. of Biomedical Sciences and Human Oncology, University of Bari Aldo Moro, Bari, Italy

***Corresponding Author at**: Dept. of Biomedical Sciences and Human Oncology, University of Bari Aldo Moro, Bari, Italy jeanfrancois.desaphy@uniba.it

Running title: Myotonic Nav1.4 variant pharmacogenetics

Declarations of Interest: None

Funding: This study was supported by grant GGP14096 from Telethon-Italy (non-profit).

Abstract

Sodium channel myotonia and paramyotonia congenita are caused by gain-of-function mutations in the skeletal muscle voltage-gated sodium channel hNav1.4. The first-line drug is the sodium channel blocker mexiletine; however, some patients show side effects or limited responses. We previously showed that two hNav1.4 mutations, p.G1306E and p.P1158L, reduce mexiletine potency in vitro, whereas another sodium channel blocker, flecainide, is less sensitive to mutation-induced gating defects. This observation was successfully translated to p.G1306E and p.P1158L carriers. Thus, the aim of this study was to perform a pharmacological characterization of myotonic Nav1.4 mutations clustered near the fast inactivation gate of the channel. We chose seven mutations (p.V1293I, p.N1297S, p.N1297K, p.F1298C, p.G1306E, p.I1310N, and p.T1313M) from the database of Italian and French networks for muscle channelopathies. Recombinant hNav1.4 mutants were expressed in HEK293T cells for functional and pharmacological characterization using the patch-clamp technique. All the studied mutations impair the kinetics and/or voltage dependence of fast inactivation, which is likely the main mechanism responsible for myotonia. The severity of myotonia is well-correlated to the enhancement of window currents generated by the intersection of the activation and fast inactivation voltage dependence. Five of the six mutants displaying a significant positive shift of fast inactivation voltage dependence reduced mexiletine inhibition in an experimental condition mimicking myotonia. In contrast, none of the mutations impairs flecainide block nor does p.T1313M impair propafenone block, indicating that class Ic antiarrhythmics may constitute a valuable alternative. Our study suggests that mutation-driven therapy would be beneficial to myotonic patients, greatly improving their quality of life.

Keywords: myotonia; sodium channel; mexiletine; flecainide; propafenone

1. Introduction

Dominantly inherited missense mutations in the *SCN4A* gene encoding the skeletal muscle voltage-gated sodium channel Nav1.4 are responsible for sodium channel myotonia (OMIM 608390) and paramyotonia congenita (OMIM 168300) [1-3]. Myotonic mutations have been found throughout the entire *SCN4A* coding region but are more frequent in the channel structures involved in voltage sensing and fast inactivation. Indeed, most mutations produce a gain of function of the sodium channel through alteration of the kinetics and/or voltage dependence of fast inactivation that normally develops on a timescale of a few milliseconds. Only a few mutations have been shown to enhance activation. Gain of function of the sodium channel increases sarcolemma excitability, which leads to muscle stiffness. The impairment of slow inactivation, which normally develops in tens of seconds, is generally associated with an increased propensity of episodes of muscle weakness leading to flaccid paralysis in patients.

Sodium channel blockers have been empirically used to treat myotonia because they reduce abnormal action potential firing in myofibers. A clinical trial confirmed the effectiveness of the class Ib antiarrhythmic mexiletine in myotonic patients [4], and today, this drug is preferred in many countries [5]. However, about one-third of patients are intolerant or report an unsatisfactory response to mexiletine [1, 6]. In previous studies, we and others have questioned the sensitivity of myotonic sodium channel mutants to mexiletine [7-8]. It was observed that the mutations located in the segment S6 of domain IV of the channel, which contributes to the binding site for mexiletine, may allosterically modify the sensitivity of the channel to the drug [7]. In addition, mutations located elsewhere in the channel may modify channel gating in a manner that secondarily affects apparent drug affinity [8]. Thus, we found that the p.G1306E mutation that causes severe myotonia permanens induces a pronounced depolarizing shift of fast inactivation, which

significantly impairs mexiletine block [8]. Interestingly, the p.G1306E mutant conserves the same sensitivity as the wild-type (WT) channel to the class Ic antiarrhythmic flecainide likely because flecainide preferentially binds to open channels [9]. Accordingly, myotonic p.G1306E carriers usually show limited response to mexiletine but obtain great improvement with flecainide [10-11]. A mexiletine-to-flecainide shift was also successful in treating a young girl carrying p.P1158L, which evokes functional defects similar to p.G1306E [12]. These results provided a basis for precision medicine in myotonic syndromes using a mutation-driven therapy aimed at increasing efficacy and reducing side effects [13].

Thus, the principal aim of the current study was to perform a pharmacological characterization of myotonic Nav1.4 variants. We focused on mutations close to p.G1306E, which belong to the intracellular linker between domain III and IV, which is mechanistically responsible for fast inactivation, and the neighboring sixth segment of domain III. The linker constitutes the hinge lid that may bind to the intracellular mouth of the pore and stops ion conduction [14]. A recent alternative hypothesis suggested by cryo-electron microscopy data consists of an allosteric blocking mechanism through the binding of the inactivation particle to a hydrophobic cavity formed by S4-S5 linkers and S6 segments in domains III and IV [15]. Seven mutations (p.V1293I, p.N1297S, p.N1297K, p.F1298C, p.G1306E, p.I1310N, and p.T1313M) were identified in the database of Italian and French networks for skeletal muscle channelopathies, and relative clinical information was collected. We performed patch-clamp experiments on recombinant mutant channels in an attempt to correlate the biophysical defects to the patients' symptoms and to verify sensitivity to mexiletine and flecainide. The results indicate that the voltage dependence of fast inactivation is the main determinant of mutant channel sensitivity to mexiletine and that flecainide may constitute a valuable alternative to mexiletine.

2. Materials and Methods

2.1. Human studies

Myotonic cases were extracted from the database of networks on skeletal muscle ion channelopathies from France (Resocanaux) and Italy (Italian Association of Myology), where genetic diagnoses were performed after obtaining written informed consent signed by the patients in accordance with the Helsinki Declaration. Seven mutations were chosen because they are located in the intracellular linker between domains III and IV of the sodium channel protein, which contains the fast inactivation particle. Clinical and neurological data of the mutation carriers obtained in our clinics include a description of myotonic symptoms, occurrence of weakness and/or pain, severity of symptoms, and pharmacological treatments.

2.2 Heterologous expression of sodium channel variants

The mutations were introduced into the pRc/CMV-hNav1.4 vector containing the full-length cDNA encoding the wild-type (WT) human skeletal muscle voltage-gated sodium channel, using the QuikChange Lightning Site-Directed Mutagenesis kit (Agilent Technologies, Santa Clara, CA) and were confirmed by complete sequencing. The HEK293T cells (Sigma-Aldrich) were grown following standard procedures in Dulbecco's MEM culture medium. During passages 3 to 10, the cells were cotransfected with WT or mutated pRc/CMV-hNav1.4 (0.5 µg/mL) and pCD8-IRES-hβ1 (0.1 µg/mL) expressing the sodium channel auxiliary β1 subunit and the CD8 receptor gene reporter, using the calcium-phosphate coprecipitation method, as previously described [12, 16]. Thirty-six to

96 hours after transfection, cells marked by anti-CD8 antibody-coated microbeads (Dynal-Invitrogen, Milan, Italy) were used for patch-clamp experiments.

2.3 Patch-clamp experiments

Whole-cell sodium currents were recorded using Axopatch 1D patch-clamp amplifier (Axon Instruments, Union City, CA) at room temperature (20–22 °C), as previously described [12, 16-17]. The composition of the pipette solution was 120 mM CsF, 10 mM CsCl, 10 mM NaCl, 5 mM EGTA and 5 mM Cs-HEPES (pH 7.2). The bath solution contained 150 mM NaCl, 4 mM KCl, 2 mM $CaCl_2$, 1 mM $MgCl_2$, 5 mM Na-HEPES and 5 mM glucose (pH 7.4). The resistance of the patch pipettes ranged from 1.5 to 3.0 MΩ. The capacitance currents and series resistances were partially compensated using the amplifier circuit. Only data obtained in cells displaying series resistance errors < 5 mV were considered for analysis. The recordings were low-pass filtered at 2 kHz (-3 dB) by the four pole Bessel filter of the amplifier.

The voltage clamp protocols are described in the Results section and figures. Mexiletine hydrochloride, propafenone hydrochloride, and flecainide-acetate salt (Sigma-Aldrich, Milan, Italy) were solubilized in the bath solution at the final concentration. The patched cell was exposed to a continuous gravity-driven stream of control or drug-supplemented bath solution. Because of the known spontaneous shift of voltage dependence during whole-cell experiments, the various protocols were applied respecting a constant sequence to allow comparison between the cells, and a maximum of two drug concentrations were tested on each cell [12, 16-17].

Data analysis was performed using pCLAMP 10.3 (Axon Instruments) and SigmaPlot 8.02 (Systat Software GmbH, Erkrath, Germany). The voltage dependence of fast inactivation was fitted to a Boltzmann equation:

$$I / I_{max} = 1 / \{1 + \exp([V - fV_{50}] / Kf)\} \quad (1)$$

where fV_{50} is the half-maximum voltage of fast inactivation and Kf is the slope factor. Because some of the channels do not enter slow inactivation, a residual current, I_R, was introduced in the equation to fit the voltage dependence of slow inactivation:

$$I / I_{max} = I_R + (1-I_R) / \{1 + \exp([V - sV_{50}] / Ks)\} \quad (2)$$

where sV_{50} is the half-maximum voltage of slow inactivation and Ks is the slope factor.

The full drug concentration-effect relationships were constructed from data obtained in different cells challenged with no more than two drug concentrations and were fitted to a first-order binding function:

$$I_{DRUG} / I_{CONTROL} = 1 / \{1 + ([drug] / IC_{50})^{nH}\} \quad (3)$$

where IC_{50} is the half-maximum inhibitory concentration and nH is the Hill coefficient. The fit parameters of concentration-effect relationships are given with the standard error (SE) of the regression.

2.4 Statistical analysis

The data are reported as the mean ± standard error of the mean (SEM) from n cells. For the statistical analysis of voltage dependence, a complete relationship was constructed in each cell and the fit parameters were averaged as the mean ± SEM from n cells. The comparison of WT and sodium channel variants was performed using ANOVA followed by two-tailed Bonferroni's t test, with $p < 0.05$ considered as significant.

3. Results

3.1 Clinical and genetic evaluations

We report the clinical symptoms and genetics of myotonic patients carrying mutations located at evolutionary-conserved positions in the inactivation gate of the hNav1.4 sodium channel (Supplementary Fig. 1). The patients were identified by the network for muscle channelopathies of the Italian Association of Myology, with the exception of p.N1297K and p.I1310N, which were identified by the French network for muscle channelopathies (Resocanaux). The mutations were *de novo* or dominantly inherited. The clinical and genetic features are summarized in Table 1. A more detailed description can be found in the supplementary material.

p.V1293I (c.3877G>A): The p.V1293I mutation was found in two unrelated individuals of the Italian database, likely occurring *de novo* in one case and dominantly inherited in the other, both with onset during the third decade. One patient was referred with mild symptoms of sodium channel myotonia. She took 200 mg/day mexiletine for 20 days but discontinued treatment because she experienced worsening muscle stiffness. Because of the mild symptoms, she did not take any further treatment. The other patient showed symptoms of paramyotonia congenita of moderate intensity and responded well to mexiletine 200 mg bid.

The same mutation was reported by others to be associated with various clinical manifestations ranging from sodium channel myotonia to paramyotonia congenita and paralysis [18-22]. Two patients carrying p.V1293I showed significant improvement with mexiletine at doses of 400 and 600 mg/day [22-23].

p.N1297S (c.3890A>G): This novel mutation was found in an Italian woman and her father, both of whom also carried the p.F167L mutation in *CLCN1* encoding the ClC-1 chloride channel. Clinical symptoms have been recently reported [24]. Briefly, the proband presented with painful stiffness in limbs and occasional episodes of transient weakness.

The father reported mild and painful muscle stiffness in the hands, without weakness episodes. The patients did not take any drugs for myotonia.

p.N1297K (c.3891C>A): The mutation was detected *de novo* in a baby girl suffering from severe neonatal nondystrophic myotonia, and clinical symptoms were previously reported [25]. The child was treated first with carbamazepine without any improvement, then with mexiletine with relatively good but unsustained improvement. She died at 20 months of age from a prolonged respiratory arrest during a bronchopulmonary infection.

p.F1298C (c.3893T>G): This is a new mutation found in a 35-year-old female suffering from painful, cold-sensitive myotonia without weakness. The patient was administered mexiletine (400 mg/day), which was discontinued due to poor tolerance, although improvements in myotonia were reported. The patient's father, who carried the same mutation, was asymptomatic and did not take any medication for myotonia.

p.G1306E (c.3917G>A): The mutation has been found in 7 patients from 6 pedigrees in the Italian database. It is generally associated with neonatal stridor or SNEL and with a very severe myotonic phenotype in adulthood, which can be painful and can greatly interfere with development and quality of life. Episodic weakness has never been reported. A comprehensive review of p.G1306E carriers, including some Italian individuals, has recently been published [11]. The patients generally obtain little improvement with mexiletine. Based on our in vitro studies [8- 9], flecainide (100 mg bid in adults) is now the preferred drug for p.G1306E carriers [10-11, 26].

p.I1310N (c.3929T>A): The mutation was found in 5 members of a single kindred and was previously included in an EMG study [19]. The age of onset is variable, ranging from 2 to

50 years. The patients report exercise and cold-aggravated myotonia of moderate-to-severe intensity. They do not take any medications for myotonia.

p.T1313M (c.4015C>T): This mutation is one of the most common associated with paramyotonia congenita plus periodic paralysis, at least in Europe [20, 27-28]. Accordingly, eleven carriers from five unrelated pedigrees are reported in the Italian Network database. Some patients do not take any medications for myotonia, while others take mexiletine (600-1000 mg/day). Several p.T1313M carriers with limited improvement and intolerable side effects with mexiletine have been reported [23, 29-31]. Conversely, three related Japanese carriers obtained significant improvement of symptoms with 400/600 mg/day mexiletine [32]. Long-term therapy with flecainide (200 mg/day) has proven successful in p.T1313M carriers from a large pedigree [31].

3.2 Functional study of hNav1.4 myotonic variants

The seven mutations were introduced into hNav1.4 cDNA by site-directed mutagenesis and were expressed in HEK293T cells for whole-cell patch-clamp recording. The functional effects of p.N1297S have been shown in a recent study [24] and some are reported here to allow direct comparison. Although p.G1306E was previously reported [8], experiments were repeated in this study to have a complete picture of functional defects allowing direct comparison.

All the expressed mutants conducted sodium currents with rapid activation and inactivation (Fig. 1A). The current-voltage relationships were well superimposed for all the mutants except for F1298C, which presented a positive ~20 mV shift of the entire curve (Fig. 1B). The voltage dependence of activation, derived from I-V relationships are shown in Supplementary Fig. 2, and Boltzmann fit parameter values are reported in

Supplementary Table 1. Only p.F1298C showed a significantly different half-maximum activation voltage, which was shifted toward a less negative voltage by 19.6 mV compared to WT. The steepness of the voltage dependence was significantly lower for p.F1298C, p.N1297K, and p.I1310N.

The sodium current decay was fitted to a monoexponential function to evaluate the velocity of channel entry into the inactivated state, as shown in Supplementary Fig. 3. Except for p.N1297S, all the channel mutants inactivated more slowly that WT, as indicated by the longer time constant of current decay (Fig. 1C). This defect was more pronounced for p.F1298C and p.G1306E, followed by p.T1313M, then by p.V1293I, p.N1297K, and p.I1310N.

The voltage dependence of steady-state fast inactivation was evaluated by using a conventional two-pulse voltage clamp protocol (Fig. 2A). The peak sodium current amplitude measured during the test pulse was normalized and was reported as a function of conditioning 50 ms-long pulse voltage. The relationships were fitted to a Boltzmann equation, and fit parameter values are reported in Table 2. All the mutants significantly shifted the half-maximum inactivation voltage (fV_{50}) value toward a less negative voltage ($P<0.0001$ *versus* WT with ANOVA followed by Bonferroni's t test), with the exception of p.V1293I ($P=0.06$) (Fig. 2b). The shift was greater for p.F1298C and p.G1306E (approximately 17 mV) than for p.T1313M and p.I1310N (approximately 11 mV) or for p.N1297S and p.N1297K (approximately 6 mV).

The overlap of activation and fast inactivation defines a window of potentials at which the probability of channels opening is higher. The area delimited by the intersection of activation and fast inactivation relationships defines the window current. As an example, window currents for the WT and p.G1306E hNav1.4 channels are illustrated in Fig. 2C. The window currents of the other myotonic hNav1.4 variants are shown in Supplementary Fig. 4. Compared to WT, all the variants are likely to open within a larger window of

membrane potentials. In particular, p.V1293I, p.N1297K, p.G1306E, p.I1310N, and p.T1313M would need less membrane depolarization to open, thereby greatly enhancing cell excitability. For p.N1297S and p.F1298C, the open probability is increased only at less negative potentials. The areas beneath the curve were calculated to quantify window currents and are reported in Fig. 2D. All the myotonic variants displayed window currents greater than WT, the effect being more pronounced for p.G1306E, p.N1297K, and p.V1293I, than for p.I1310N and p.T1313M or for p.F1298C and p.N1297S.

In addition to fast inactivation, sodium channels enter a slow inactivated state that develops on a time scale of seconds [33]. We measured the voltage dependence of slow inactivation by using a conditioning pulse lasting 30 s and by introducing an intermediate hyperpolarized pulse of 20 ms to allow recovery from fast inactivation before assessing the availability of the channel to open (Fig. 3A). The peak sodium current amplitude measured during the test pulse was normalized and was reported as a function of conditioning 30 s-long pulse voltage. The relationships were fitted to a Boltzmann equation containing a residual current because approximately 30 % of channels did not inactivate at positive voltages (Fig. 3B), and fit parameters are reported in Table 2. The p.T1313M mutation had no significant effect on slow inactivation. The p.N1297S mutation did not significantly affect the half-maximum inactivation voltage (sV_{50}); however, it reduced the maximal number of inactivating channels [24]. The other mutations enhanced slow inactivation by shifting sV_{50} toward more negative voltages and/or by increasing the maximal number of inactivating channels (Fig. 3C and D).

3.3 Pharmacological study of hNav1.4 myotonic variants

Mexiletine was tested on all the mutants using a protocol allowing direct comparison with previous data [8-9, 12]. The holding potential was -120 mV, and 20 ms-long test

pulses at -30 mV were applied every 10 seconds (0.1 Hz) or 0.1 seconds (10 Hz) to evaluate tonic and phasic block, respectively. Representative sodium current traces and concentration-response relationships are shown in Fig. 4, with fit parameter values reported in Table 2. Using this protocol, the p.V1293I variant showed sensitivity to mexiletine similar to WT, as previously reported [7]. In contrast, all the other variants showed reduced sensitivity to mexiletine compared to WT. For all the mutants, this effect was more pronounced at 10 Hz, with the fold reduction of the half-maximum inhibitory concentration (IC_{50}) ranging from 2.3 for p.F1298C to 6.0 for p.N1297S (Table 3).

In previous studies, we showed that flecainide apparent affinity is less affected by some sodium channel mutations, which eventually was successfully translated to mutation carriers [9-12]. Thus, we performed the same experiments with flecainide, except for p.V1293I. The results are illustrated in Fig. 5, and the fit parameter values are presented in Table 2. Four mutant channels (p.N1297S, p.N1297K, p.F1298C, and p.G1306E) showed flecainide sensitivity similar to WT at both stimulation frequencies. The two other mutations, p.I1310N and p.T1313M, displayed an increased sensitivity to flecainide; the most dramatic effect was observed with p.I1310N at 10 Hz, with an ~4-fold reduction in the IC_{50} value.

Myotonic discharges are characterized by action potential firing at frequencies of tens to hundreds Hz. To measure drug effects in a condition more similar to a myotonic discharge, we applied 5 ms-long depolarizing test pulses at a frequency of 50 Hz from a holding potential of -90 mV (close to muscle membrane resting voltage). In these conditions, in the absence of drug, the sodium current amplitude decreased because of the failure of some of the channels to recover from inactivation between two depolarizing pulses (Supplementary Fig. 5). Thus, WT currents showed a use-dependent decrease reaching 34.5 ± 2.7 % (n=40) in 4 seconds. This reduction was only 22.8 ± 1.9 % for p.N1297S (n=35, $P<0.0001$); however, it was greatly enhanced to 55.5 ± 4.2 % for

p.I1310N (n=17, P<0.0001). The addition of drug produces a tonic block (TB) measured at a stimulation frequency of 0.1 Hz. Representative sodium current traces generated by WT and p.G1306E variants are illustrated in Fig. 6A, showing a use-dependent block at 50 Hz in the absence of drug (UDB-c), a tonic block exerted by 30 µM mexiletine, and a use-dependent block in the presence of drug (UDB-d). As previously described in detail [34-35], UDB-d was corrected for UDB-c to obtain the net use-dependent effect of drug on sodium channel variants. This latter was added to TB to obtain the percentage of block exerted by the drugs, which is reported for mexiletine and flecainide in Fig. 6B and C. The variants p.N1297K, p.F1298C, p.G1306E, p.I1310N, and p.T1313M, all reduced blockade by mexiletine, and this effect was significant at 3, 10, and 30 µM. The two other variants, p.V1293I and, more surprisingly, p.N1297S, did not affect mexiletine blockade. In contrast, none of the myotonic variants significantly affected flecainide blockade.

Propafenone was reported to be highly effective in a p.T1313M carrier intolerant to mexiletine [29]. We thus tested propafenone on WT and p.T1313M sodium currents (Supplementary Fig. 6A and B). With IC_{50} values of 18 and 3 µM for the inhibition of wild-type channels at 0.1 and 10 Hz, respectively, propafenone appeared more potent than mexiletine and flecainide at both frequencies (Table 3). The drug exerted a similar effect on p.T1313M channels. Similarly, in myotonia-like conditions, propafenone exerted the same inhibitory effect on WT and p.T1313M variants (Supplementary Fig. 6C and D).

4. Discussion

In this study, we reported the functional and pharmacological characterization of seven myotonic hNav1.4 mutations located near the fast inactivation gate of the sodium channel. These mutations are associated with different myotonic phenotypes with various levels of severity.

All the variants impaired fast inactivation, which is likely the main mechanism underlying myotonia. Five mutations combine two defects, which are slower entry into fast inactivation and positive shift of fast inactivation voltage dependence. Two mutations, p.V1293I and p.N1297S, affect only one of these parameters. Accordingly, the latter are associated with milder phenotypes in our database. However, p.V1293I is notoriously associated with a great variety of phenotypes, suggesting that the mutation is also particularly influenced by modifier genes and/or environmental conditions [18-22]. In p.N1297S carriers, the simultaneous occurrence of a mutation in the ClC-1 chloride channel may also influence the phenotype [24]. The p.I1310N and p.T1313M variants have moderate effects on fast inactivation parameters, which account well for the clinical phenotype. Both the p.F1298C and p.G1306E variants show the most dramatic effects on fast inactivation kinetics and voltage dependence. Accordingly, the p.G1306E carriers all present a severe phenotype of myotonia permanens, which is often associated with neonatal symptoms. In contrast, the p.F1298C proband presented with mild to moderate symptoms, and her father showed a benign phenotype. It is noteworthy that the positive shift of activation voltage dependence induced by p.F1298C may mitigate the effects of fast inactivation impairment. Finally, the mild effects of p.N1297K on fast inactivation parameters are not sufficient to support the apparent severity of the case [25].

Interestingly, the window currents appeared more predictive of phenotype severity. Thus, the two mutations with the greater window current areas, p.G1306E and p.N1297K, are the most clinically severe. The two mutations with the minor window current areas, p.N1297S and p.F1298C, are associated with milder phenotypes. The mutations p.V1293I, p.I1310N, and p.T1313M, showing mid-range window current areas, are usually associated with a moderate phenotype.

Several mutations also affect slow inactivation. Impairment of slow inactivation has been generally associated with the increased propensity of long-lasting paralytic attacks in

myotonic patients [33, 36-37]. The impairment of slow inactivation by p.N1297S is not sufficient to evoke episodic paralysis in the carriers, probably because other functional defects are not sufficiently dramatic considering the lack of a defect in the rate for entry into fast inactivation [24]. Among the mutations studied here, episodic weakness has been reported by others for p.V1293I and p.T1313M [29, 32]. Both mutations showed no effect on slow inactivation voltage dependence, as previously reported [38-39], while p.V1293I enhanced maximal slow inactivation at depolarized voltages. These data suggest that slow inactivation may have little relevance for paralysis induced by these two mutations, although we cannot exclude its effects on the development of slow inactivation and recovery rates or the specific effects of cold or hyperkalemia on slow inactivation. Regarding p.N1297K, p.F1298C, p.G1306E, and p.I1310N, the enhancement of slow inactivation may explain the lack of paralytic attacks in the patients, especially in the more severe cases of myotonia permanens. Apparently, slow inactivation enhancement cannot prevent myotonia.

Structurally, impairment of slow inactivation by amino acid substitutions in the inactivation gate may appear surprising since many studies suggested that slow inactivation involves amino acids in the filter selectivity and surrounding S5 and S6 segments [14]. However, removal of fast inactivation by substitution of the IFM triplet within the DIII-DIV linker was shown to accelerate and accentuate slow inactivation, suggesting that fast inactivation may affect the development of subsequent slow inactivation [40]. In our study, there was no correlation between the voltage dependent shifts of fast and slow inactivation: p.V1293I did not shift fV_{50} but positively shifted sV_{50}; on the other hand, p.T1313M positively shifted fV_{50} but did not affect sV_{50}. The effects on slow inactivation voltage dependence of mutations in the fast inactivating particle was thus mutation-specific, suggesting that these mutations may exert specific allosteric effects on

slow inactivation machinery, likely when the fast inactivation particle is positioned in the inactivated state.

Mexiletine is today the preferred option for alleviating myotonia [4, 6, 41]. However, a number of patients remain unsatisfied with the drug due to poor response or side effects. Mexiletine inhibits sodium channels by binding to the local anesthetic receptor located within the pore of the channel, and its effects are largely dependent on channel gating [16-17]. Thus, channel mutations close to the binding site or altering the gating may influence mexiletine block [7-9]. The main objective of the present work was to verify the mexiletine sensitivity of myotonic sodium channel mutations located near the inactivation gate of the channel. The results indicate that the voltage dependence of fast inactivation is critical for defining channel sensitivity to mexiletine, as suggested previously [8-9, 12]. Only p.V1293I, which has an fV_{50} value similar to WT, shows IC_{50} values at 0.1 and 10 Hz similar to WT. All the other variants display a positive shift of fV_{50} and a reduced apparent affinity to mexiletine. It is worth noting that we previously showed that the p.G1306E variant does not affect binding of mexiletine to its receptor, supporting the hypothesis than the gating defect causes the reduction of inhibition [8]. Although we cannot exclude that some variants may affect binding of the drug through allosteric interactions of the mutated amino acid with the local anesthetic receptor, especially when the inactivation gate closes the pore, some studies suggest that fast inactivation gate movement is not affected by drug binding [42]. Thus, it is likely that the preferential binding of mexiletine to fast inactivated channels is mostly contrasted by the positive shift of fast inactivation voltage dependence that reduces the proportion of inactivated channels at negative voltages. The threshold of the fV_{50} shift to alter mexiletine sensitivity is positioned between 3.5 (V1293I) and 6 mV (N1297K). However, there is no linear correlation between the IC_{50} and fV_{50} values (not shown). For instance, p.N1297S and p.N1297K display a similar fV_{50} shift, but p.N1297S is about two fold less sensitive to mexiletine. Conversely, p.N1297S and

p.G1306E show the same sensitivity to mexiletine, while the fV_{50} for G1306E is 10 mV less negative than for p.N1297S. This observation suggests that the voltage dependence of fast inactivation is not the sole determinant of mexiletine apparent affinity. Mexiletine can act as an open channel blocker, at least in inactivation-deficient channels [43] and may interact with slow inactivation [44]. Thus, aside from the key role of fast inactivation voltage dependence, it is likely that the complex alteration of sodium channel gating specific to each myotonic mutation may further influence the sensitivity to mexiletine in an individual manner. The effects of mexiletine measured in a myotonia-like condition at 50 Hz largely confirmed the results obtained at lower frequencies and more negative holding potentials. A striking exception is p.N1297S, which was as sensitive as WT to mexiletine at 50 Hz. Because p.N1297S is the only variant with unchanged fast inactivation kinetics, it is possible that such parameter may assume a critical role for drug sensitivity during high-frequency firing. p.N1297S is also the only variant showing reduction of slow inactivation. It is worth noting that mexiletine effects in myotonia-like conditions were observed at concentrations close to the therapeutic level in blood.

In rats with chloride channel myotonia, flecainide exerts antimyotonic activity at lower doses compared to mexiletine [35]. This activity may rely on different pharmacokinetics and/or different molecular effects on sodium channels [45]. Importantly, the present data suggest that the flecainide advantage would not be lost in sodium channel myotonia because mutations do not impair channel inhibition by the drug and may even increase its sensitivity in some cases. It is widely acknowledged that, compared to class Ib antiarrhythmic drugs such as mexiletine, class Ic antiarrhythmics such as flecainide bind preferentially to open channels and are less dependent on fast inactivation gating. Thus, the shift of inactivation voltage dependence by sodium channel variants would have less influence on flecainide effects, as confirmed by our data. This hypothesis is further supported by the effects of propafenone on p.T1313M, another class Ic antiarrhythmic.

Translation of in vitro pharmacogenetics to humans may be possible. Our hypothesis is that, in the heterozygous patient carrying a sodium channel mutation inducing a right shift of inactivation voltage dependence, the effects of mexiletine may largely rely on the inhibition of wild-type channels, with limited efficacy. This implies that patients would require higher doses of mexiletine to gain benefits, exposing themselves to higher risks of side effects and intolerance. Our study indicates that flecainide, and probably other class Ic antiarrhythmics, such as propafenone, constitute a valuable therapeutic option in the case of an unsatisfactory response to mexiletine. Translation from the lab bench to bedside was indeed successful for p.G1306E, p.P1158L, and p.T1313M carriers [10-12, 26, 31]. Flecainide has been proven safe for most myotonic patients, even when it is used for a long period; however, side effects remain possible. Recently, a p.G1306E carrier taking 200 mg flecainide a day developed symptoms of syncope and palpitation with a Brugada ECG pattern [46]. Therefore, the patient reverted to the previous treatment regimen of 1,200 mg mexiletine per day, which is twice the recommended daily dose.

Our study suggests that a mutation-driven therapy would be beneficial to myotonic patients, greatly improving their quality of life. Such a hypothesis would need to be verified in a head-to-head clinical trial of flecainide *versus* mexiletine. Now, we can only propose that flecainide may be a valuable therapeutic option in case of unsatisfactory response to mexiletine. Pharmacogenetics studies may also be extended to other sodium channel mutations and other potential antimyotonic drugs, such as lamotrigine [47], ranolazine [48], riluzole [35], or new derivatives [34]. Recently reported death events in children carrying myotonic sodium channel mutations [11, 25] and associations with Sudden Infant Death Syndrome [49] both point the need to define an efficient precision medicine to avoid life-threatening events. Finally, this study may serve as a paradigm for other rare diseases related to sodium channel mutations, including epilepsy, encephalopathy, cardiac arrhythmias, and neuropathic pain [5].

Funding

This study was supported by grant GGP14096 from Telethon-Italy (non-profit).

Acknowledgements

We would like to thank the patients and their families, and the MiA association ("Miotonici in Associazione") for their participation to this study. We thank Dr. Eleonora Canioni for her technical support in molecular diagnosis at Fondazione IRCCS Istituto Neurologico Carlo Besta.

Appendix A. Supplementary data

Supplementary material related to this article can be found in the online version

References

1. J. Statland, L. Phillips, J.R. Trivedi, Muscle channelopathies. Neurol. Clin. 32 (2014) 801-815.
2. K. Suetterlin, R. Männikkö, M.G. Hanna, Muscle channelopathies: recent advances in genetics, pathophysiology and therapy. Curr. Opin. Neurol. 27 (2014) 583-590.
3. S.C. Cannon, Sodium channelopathies of skeletal muscle. Handb. Exp. Pharmacol. 246 (2018) 309-330.
4. J.M. Statland, B.N. Bundy, Y. Wang, D.R. Rayan, J.R. Trivedi, V.A. Sansone, et al., Mexiletine for symptoms and signs of myotonia in nondystrophic myotonia: a randomized controlled trial. JAMA 308 (2012) 1357-1365.
5. P. Imbrici, A. Liantonio, G.M. Camerino, M. De Bellis, C. Camerino, A. Mele, et al., Therapeutic approaches to genetic ion channelopathies and perspectives in drug discovery. Front. Pharmacol. 7 (2017) 121.
6. K.J. Suetterlin, E. Bugiardini, J.P. Kaski, J.M. Morrow, E. Matthews, M.G. Hanna, et al., Long-term safety and efficacy of mexiletine for patients with skeletal muscle channelopathies. JAMA Neurol. 72 (2015) 1531-1533.
7. M.P. Takahashi, S.C. Cannon, Mexiletine block of disease-associated mutations in S6 segments of the human skeletal muscle Na(+) channel. J. Physiol. 537 (2001) 701-714.
8. J.F. Desaphy, A. De Luca, P. Tortorella, D. De Vito, A.L. George Jr., D. Conte Camerino, Gating of myotonic Na channel mutants defines the response to mexiletine and a potent derivative. Neurology 57 (2001) 1849-1857.
9. J.F. Desaphy, A. De Luca, M.P. Didonna, A.L. George Jr., D. Conte Camerino, Different flecainide sensitivity of hNav1.4 channels and myotonic mutants explained by state-dependent block. J. Physiol. 554 (2004) 321-334.

10. J.F. Desaphy, A. Modoni, M. Lomonaco, D.C. Camerino, Dramatic improvement of myotonia permanens with flecainide: a two-case report of a possible bench-to-bedside pharmacogenetics strategy. Eur. J. Clin. Pharmacol. 69 (2013) 1037-1039.
11. F. Lehmann-Horn, A. D'Amico, E. Bertini, M. LoMonaco, L. Merlini, K.R. Nelson, et al., Myotonia permanens with Na1.4-G1306E displays varied phenotypes during course of life. Acta Myol. 36 (2017) 125-134.
12. J.F. Desaphy, R. Carbonara, A. D'Amico, A. Modoni, J. Roussel, P. Imbrici, et al., Translational approach to address therapy in myotonia permanens due to a new SCN4A mutation. Neurology 86 (2016) 2100-2108.
13. M. De Bellis, D.C. Camerino, J.F. Desaphy, Toward precision medicine in myotonic syndromes. Oncotarget 8 (2017) 14279-14280.
14. T.M. Gamal El-Din, M.J. Lenaeus, W.A. Catterall, Structural and Functional analysis of sodium channels viewed from an evolutionary perspective. Handb. Exp. Pharmacol. 246 (2018) 53-72.
15. X. Pan, Z. Li, Q. Zhou, H. Shen, K. Wu, X. Huang, et al., Structure of the human voltage-gated sodium channel Nav1.4 in complex with β1. Science 2018 Sep 6. pii: eaau2486. doi: 10.1126/science.aau2486. [Epub ahead of print]
16. J.F. Desaphy, A. Dipalma, M. De Bellis, et al., Involvement of voltage-gated sodium channels blockade in the analgesic effects of orphenadrine. Pain 142 (2009) 225-235.
17. J.F. Desaphy, A. Dipalma, T. Costanza, R. Carbonara, M.M. Dinardo, A. Catalano, et al., Molecular insights into the local anesthetic receptor within voltage-gated sodium channels using hydroxylated analogs of mexiletine. Front. Pharmacol. 3 (2012) 17.
18. M.C. Koch, K. Baumbach, A.L. George, K. Ricker, Paramyotonia congenita without paralysis on exposure to cold: a novel mutation in the SCN4A gene (Val1293Ile). NeuroReport 6 (1995) 2001-2004.

19. E. Fournier, K. Viala, H. Gervais, D. Sternberg, M. Arzel-Hézode, P. Laforêt, et al., Cold extends electromyography distinction between ion channel mutations causing myotonia. Ann. Neurol. 60 (2006) 356-365.
20. A. Horga, D.L. Raja Rayan, E. Matthews, R. Sud, D. Fialho, S.C. Durran, et al., Prevalence study of genetically defined skeletal muscle channelopathies in England. Neurology 80 (2013) 1472-1475.
21. K.W. Chung, D.H. Yoo, S.J. Lee, B.O. Choi, S.S. Lee, A large dominant myotonia congenita family with a V1293I mutation in SCN4A. J. Clin. Neurol. 12 (2016) 509-511.
22. A. Magot, A. David, D. Sternberg, Y. Péréon, Focal and abnormally persistent paralysis associated with congenital paramyotonia. BMJ Case Rep. 2014 Jun 17;2014. pii: bcr2014204430. doi: 10.1136/bcr-2014-204430.
23. F. Al-Ghamdi, B.T. Darras, P.S Ghosh, Spectrum of nondystrophic skeletal muscle channelopathies in children. Pediatr. Neurol. 70 (2017) 26-33.
24. L. Maggi, S. Ravaglia, A. Farinato, R. Brugnoni, C. Altamura, P. Imbrici et al., Coexistence of CLCN1 and SCN4A mutations in one family suffering from myotonia. Neurogenetics 18 (2017) 219-225.
25. S. Gay, D. Dupuis, L. Faivre, A. Masurel-Paulet, M. Labenne, M. Colombani, et al., Severe neonatal non-dystrophic myotonia secondary to a novel mutation of the voltage-gated sodium channel (SCN4A) gene. Am. J. Med. Genet. A 146A (2008) 380-383.
26. S. Portaro, C. Rodolico, S. Sinicropi, O. Musumeci, M. Valenzise, A. Toscano, Flecainide-Responsive Myotonia Permanens With SNEL Onset: A New Case and Literature Review. Pediatrics 137 (2016). doi: 10.1542/peds.2015-3289.

27. E. Matthews, S.V. Tan, D. Fialho, M.G. Sweeney, R. Sud, A. Haworth, et al., What causes paramyotonia in the United Kingdom? Common and new SCN4A mutations revealed. Neurology 70 (2008) 50-53.
28. B.C. Stunnenberg, J. Raaphorst, J.C.W. Deenen, T.P. Links, A.A. Wilde, D.J. Verbove, et al., Prevalence and mutation spectrum of skeletal muscle channelopathies in the Netherlands. Neuromuscul. Disord. 28 (2018) 402-407.
29. E. Alfonsi, I.M. Merlo, M. Tonini, S. Ravaglia, R. Brugnoni, A. Gozzini, et al., Efficacy of propafenone in paramyotonia congenita. Neurology 68 (2007) 1080-1081.
30. T. Fukukome, H. Izumoto, H. Goto, H. Matsuo, T. Yoshimura, S.I. Sakoda, et al., Paramyotonia congenita due to a de novo mutation: a case report. Muscle Nerve 28 (2003) 232–235.
31. C. Terracciano, O. Farina, T. Esposito, L. Lombardi, F. Napolitano, P. Blasiis, et al., Successful long-term therapy with flecainide in a family with paramyotonia congenita. J. Neurol. Neurosurg. Psychiatry. 2018 Feb 27. doi: 10.1136/jnnp-2017-317615. [Epub ahead of print]
32. M. Kinoshita, R. Sasaki, T. Nagano, A. Matsuda, S. Nakamura, M. Takahama, et al., Thr11313Met mutation in skeletal muscle sodium channels in a Japanese family with paramyotonia Congenita. Intern. Med. 42 (2003) 856-861.
33. T.R. Cummins, F.J. Sigworth, Impaired slow inactivation in mutant sodium channels. Biophys. J. 71 (1996) 227-236.
34. M. De Bellis, R. Carbonara, J. Roussel, A. Farinato, A. Massari, S. Pierno, et al., Increased sodium channel use-dependent inhibition by a new potent analogue of tocainide greatly enhances in vivo antimyotonic activity. Neuropharmacology 113 (2017) 206-216.

35. J.F. Desaphy, R. Carbonara, T. Costanza, D. Conte Camerino, Preclinical evaluation of marketed sodium channel blockers in a rat model of myotonia discloses promising antimyotonic drugs. Exp. Neurol. 255 (2014) 96-102.
36. R.L. Ruff, Slow Na+ channel inactivation must be disrupted to evoke prolonged depolarization-induced paralysis. Biophys. J. 66 (1994) 542.
37. L.J. Hayward, G.M. Sandoval, S.C. Cannon, Defective slow inactivation of sodium channels contributes to familial periodic paralysis. Neurology 52 (1999) 1447-1453.
38. J.E. Richmond, D.E. Featherstone, P.C. Ruben, Human Na+ channel fast and slow inactivation in paramyotonia congenita mutants expressed in Xenopus laevis oocytes. J. Physiol. 499 (1997) 589-600.
39. D.S. Green, A.L. George Jr., S.C. Cannon, Human sodium channel gating defects caused by missense mutations in S6 segments associated with myotonia: S804F and V1293I. J. Physiol. 510.3 (1998) 685-694.
40. D.E. Featherstone, J.E. Richmond, P.C. Ruben, Interaction between fast and slow inactivation in Skm1 sodium channels. Biophys. J. 71 (1996) 3098-3109.
41. M. Lo Monaco, A. D'Amico, M. Luigetti, J.F. Desaphy, A. Modoni, Effect of mexiletine on transitory depression of compound motor action potential in recessive myotonia congenita. Clin. Neurophysiol. 126 (2015) 399-403.
42. V. Vedantham, S.C. Cannon, The position of the fast-inactivation gate during lidocaine block of voltage-gated Na+ channels. J. Gen. Physiol. 113 (1999) 7-16.
43. G.K. Wang, C. Russell, S.Y. Wang, Mexiletine block of wild-type and inactivation-deficient human skeletal muscle hNav1.4 Na+ channels. J. Physiol. 554.3 (2004) 621-633.
44. Y. Wang, J. Mi, K. Lu, Y. Lu, K. Wang K, Comparison of gating properties and use-dependent block of Nav1.5 and Nav1.7 channels by anti-arrhythmics mexiletine and lidocaine. PLoS One 10 (2015) e0128653.

45. F. Aoike, M.P. Takahashi, S. Sakoda, Class Ic antiarrhythmics block human skeletal muscle Na channel during myotonia-like stimulation. Eur. J. Pharmacol. 532 (2006) 24-31.
46. M. Cavalli, B. Fossati, R. Vitale, E. Brigonzi, V.A.G. Ricigliano, L. Saraceno, et al., Flecainide-induced Brugada syndrome in a patient with skeletal muscle sodium channelopathy: A case report with critical therapeutical implications and review of the literature. Front. Neurol. 9 (2018) 385.
47. G. Andersen, G. Hedermann, N. Witting, M Duno, H. Andersen, J. Vissing, The antimyotonic effect of lamotrigine in non-dystrophic myotonias: a double-blind randomized study. Brain 140 (2017) 2295-2305.
48. W.D. Arnold, D. Kline, A. Sanderson, A.A. Hawash, A. Barlett, K.R. Novak, et al., Open-label trial of ranolazine for the treatment of myotonia congenita. Neurology 89 (2017) 710-713.
49. R. Männikkö, L. Wong, D.J. Tester, M.G. Thor, R. Sud, D.M. Kullmann, et al., Dysfunction of NaV1.4, a skeletal muscle voltage-gated sodium channel, in sudden infant death syndrome: a case-control study. Lancet 391 (2018) 1483-1492.

Figure Legends

Fig. 1 Current-voltage relationships of sodium currents carried by myotonic hNav1.4 variants. (**A**) Representative sodium current traces recorded in HEK293T cells expressing WT or mutant hNav1.4 channels. Sodium currents were elicited from the holding potential of -150 mV by applying 25 ms-long test pulses from -70 to +40 mV in 10-mV intervals every 10 s. (**B**) Current-voltage relationships for WT and mutant hNav1.4 channels were determined from the sodium current traces recorded as shown in A. (**C**) Decay of sodium currents elicited between -40 and +20 mV was fit to a mono-exponential function, as shown in supplementary Fig. 3, to describe the velocity of entry into fast inactivation. Each data point is the mean ± SEM from n cells.

Fig. 2 Effects of myotonic hNav1.4 variants on fast inactivation voltage dependence and window currents. (**A**) A conventional 2-pulse voltage protocol was used to determine voltage dependence of steady-state fast inactivation. Normalized peak sodium currents measured during the test pulse at -20 mV were reported as a function of the conditioning pulse ranging from -150 to -20 mV and were applied every 10 mV. The relationships were fitted to a Boltzmann function (equation 1), and fit parameters are reported in Table 1. (**B**) The horizontal bar chart shows the shifts of half-maximum inactivation voltage (fV_{50}) ± SEM (n cells) with respect to WT. * $p<0.0001$ with ANOVA followed by two-tailed Bonferroni's *t* test. (**C**) Window currents of WT and p.G1306E obtained from the intersection of voltage dependences of activation (shown in supplementary Fig. 2) and fast inactivation. Window currents of other mutants are shown in supplementary Fig. 4. (**D**) Vertical bar graph showing window current areas for WT and myotonic hNav1.4 variants.

Fig. 3 Effects of myotonic hNav1.4 variants on slow inactivation. (**A**) Slow inactivation was induced by 30 s-long conditioning pulses. Fast inactivation was removed by an intermediate 50 ms-long pulse at -160 mV before assessing channel availability at -20 mV. (**B**) The normalized peak sodium current amplitude measured during the test pulse was reported as a function of conditioning pulse voltage. Relationships of WT and mutant channels were fitted to a Boltzmann function (equation 2), including a residual current (I_R). Fit parameter values are given in Table 1. (**C**) Horizontal bar graph showing sV_{50} shift of myotonic variants compared to WT. (**D**) Vertical bar graph displaying the maximal percentage of slow inactivated channels, calculated as [(1-I_R)·100]. Data are given as the mean ± SEM from n cells. * at least p<0.01 compared to WT with ANOVA followed by two-tailed Bonferroni's t test.

Fig. 4 Effects of mexiletine on myotonic hNav1.4 variants. (**A**) Representative WT, p.N1297K, and p.N1297S current traces recorded at steady-state before (ctrl) and during the application of 100 µM mexiletine at 0.1 and 10 Hz stimulation frequencies. Sodium currents were recorded at -30 mV from a holding potential of -120 mV. (**B**) Representative WT, pT1313M, and p.F1298C current traces recorded at steady-state before (ctrl) and during the application of 300 µM mexiletine at 0.1 and 10 Hz stimulation frequencies. (**C-D**) Concentration-effect relationships for mexiletine at 0.1 and 10 Hz were fitted to a first-order binding function (equation 3). (**E**) Horizontal bar graph showing IC_{50} values (µM) ± SE of the regression of mexiletine at 0.1 and 10 Hz.

Fig. 5 Effects of flecainide on myotonic hNav1.4 variants. (**A**) Representative WT, p.T1313M, and p.F1298C current traces recorded at steady-state before (ctrl) and during the application of 30 µM flecainide at 0.1 and 10 Hz stimulation frequencies. Sodium currents were recorded at -30 mV from a holding potential of -120 mV. (**B**)

Representative WT, p.N1297K, and p.I1310N current traces recorded at steady-state before (ctrl) and during the application of 100 µM flecainide at 0.1 and 10 Hz stimulation frequencies. (**C-D**) Concentration-effect relationships for flecainide at 0.1 and 10 Hz were fitted to a first-order binding function (equation 3). (**E**) Horizontal bar graph showing IC_{50} values (µM) ± SE of the regression of flecainide at 0.1 and 10 Hz.

Fig. 6 Effects of mexiletine and flecainide on myotonic hNav1.4 variants in myotonic-like conditions. (**A**) Representative WT and p.G1306E current traces recorded at -30 mV from a holding potential of -90 mV, at 0.1 and 50 Hz stimulation frequencies before (CTRL: 0.1 Hz; UDB-c: 50 Hz) and during the application of 30 µM mexiletine (TB: 0.1 Hz; UDB-d: 50 Hz). (**B-C**) Percentage of blocking exerted by mexiletine and flecainide on wild-type (WT) and mutant channels. Each data point is the mean ± SEM from at least 3 cells. * at least $p<0.05$ compared to WT with ANOVA followed by two-tailed Bonferroni's t test.

Table 1

Clinical properties associated to myotonic hNav1.4 mutations located close to the fast inactivation gate

Variant	Number of kindred	number of carriers	Phenotype	Age of onset	Myotonia severity	Paralysis	pain	Response to mexiletine	Current treatment
p.V1293I	1	1	SCM	24	mild	no	no	worsening	none
p.V1293I	1	1	PMC	22	moderate	no	no	good	mexiletine
p.N1297S	1	2	SCM	18	mild	mild in one	yes	*n.d.*	none
p.N1297K	1	1	SNEL	neonatal	severe	no	*n.d.*	limited	*n.d.*
p.F1298C	1	2	SCM	32	mild or asymptomatic	no	yes	good but poor tolerance	none
pG1306E	6	7	SNEL, SCM	neonatal	severe	no	yes	limited	flecainide
p.I1310N	1	5	PMC	variable [2-50 y]	moderate to severe	no	no	*n.d.*	none
p.T1313M	5	11	PMC	variable [2-48 y]	mild to severe	mild to moderate	no	variable, from limited to good	none or mexiletine

SCM: Sodium Channel Myotonia; PMC: Paramyotonia Congenita; SNEL: Severe Neonatal Episodic Laryngospasm; *n.d.*: not determined.

Table 2 Voltage-dependent parameters of myotonic hNav1.4 variants

	fast inactivation			slow inactivation			
	fV_{50} (mV)	**K_f (mV)**	**n**	**sV_{50} (mV)**	**K_s (mV)**	**I_R**	**n**
WT	-74.9 ± 0.8	5.5 ± 0.2	35	-55.9 ± 1.8	8.8 ± 0.5	0.28 ± 0.01	26
p.V1293I	-71.6 ± 1.6	6.1 ± 0.3	27	-64.3 ± 3.0[b]	7.0 ± 0.4[a]	0.21 ± 0.02[b]	18
p.N1297S	-68.2 ± 1.1[d]	5.2 ± 0.2	48	-48.2 ± 2.4[b]	8.1 ± 0.4	0.34 ± 0.01[a]	16
p.N1297K	-68.8 ± 1.1[d]	6.3 ± 0.3[a]	47	-68.3 ± 2.5[b]	5.8 ± 0.4[b]	0.23 ± 0.01[a]	13
p.F1298C	-59.2 ± 1.8[d]	7.5 ± 0.5[c]	14	-74.9 ± 1.6[d]	5.4 ± 0.5[d]	0.28 ± 0.02	20
p.G1306E	-58.5 ± 1.0[d]	6.5 ± 0.3[a]	28	-60.5 ± 1.9	8.5 ± 0.5	0.24 ± 0.02	11
p.I1310N	-65.8 ± 1.8[d]	6.6 ± 0.5[a]	16	-72.5 ± 2.2[d]	5.7 ± 1.1[c]	0.23 ± 0.02[a]	13
p.T1313M	-63.0 ± 0.9[d]	5.8 ± 0.3	47	-57.7 ± 2.7	8.5 ± 1.2	0.27 ± 0.01	11

fV_{50}, half-maximum fast inactivation voltage; K_f, fast inactivation slope factor; sV_{50}, half-maximum slow inactivation voltage; K_s, slow inactivation slope factor; I_R, residual current. Values obtained as described in Fig. 2 and 3 are reported as means ± SEM from n cells. Statistical difference versus WT was assessed using ANOVA followed by two-tailed Bonferroni's t test: [a] $p<0.05$, [b] $p<0.01$, [c] $p<0.001$, [d] $p<0.0001$.

Table 3 Half-maximum concentrations for inhibition of wild-type hNav1.4 channels and myotonic variants

Drug	Channel variant	Tonic block (0.1 Hz)		Phasic block (10 Hz)	
		IC_{50} (μM)	nH	IC_{50} (μM)	nH
Mexiletine	WT hNav1.4	256 ± 25	1.2 ± 0.1	46 ± 5	0.9 ± 0.1
	p.V1293I	220 ± 22	1.2 ± 0.1	33 ± 5	0.8 ± 0.1
	p.N1297S	691 ± 82	1.3 ± 0.2	257 ± 21	1.2 ± 0.1
	p.N1297K	493 ± 33	1.1 ± 0.1	101 ± 13	0.8 ± 0.1
	p.F1298C	356 ± 41	1.1 ± 0.1	123 ± 17	0.8 ± 0.1
	p.G1306E	662 ± 74	1.1 ± 0.2	201 ± 19	1.1 ± 0.1
	p.I11310N	507 ± 47	1.4 ± 0.2	133 ± 18	1.0 ± 0.1
	p.T1313M	598 ± 47	1.1 ± 0.1	223 ± 33	1.1 ± 0.2
Flecainide	WT hNav1.4	76 ± 7	1.2 ± 0.1	34 ± 4	1.1 ± 0.1
	p.N1297S	77 ± 9	1.1 ± 0.1	28 ± 3	1.1 ± 0.1
	p.N1297K	73 ± 6	1.2 ± 0.1	43 ± 4	1.0 ± 0.1
	p.F1298C	60 ± 6	1.2 ± 0.1	41 ± 3	1.2 ± 0.1
	p.G1306E	95 ± 13	1.0 ± 0.1	41 ± 3	1.2 ± 0.1
	p.I11310N	32 ± 4	0.8 ± 0.1	8.8 ± 0.7	0.9 ± 0.1
	p.T1313M	35 ± 5	1.1 ± 0.1	20 ± 3	1.1 ± 0.2
Propafenone	WT hNav1.4	18 ± 3	1.0 ± 0.1	3.1 ± 0.4	0.9 ± 0.1
	p.T1313M	19 ± 2	1.2 ± 0.1	3.8 ± 0.8	0.9 ± 0.2

IC_{50}, half-maximum inhibitory concentration; nH, Hill coefficient. Fit values ± SE of the fit were calculated as described in Fig. 4 and 5, and supplemental Fig. 5.

Fig. 1 (Farinato et al., 2018)

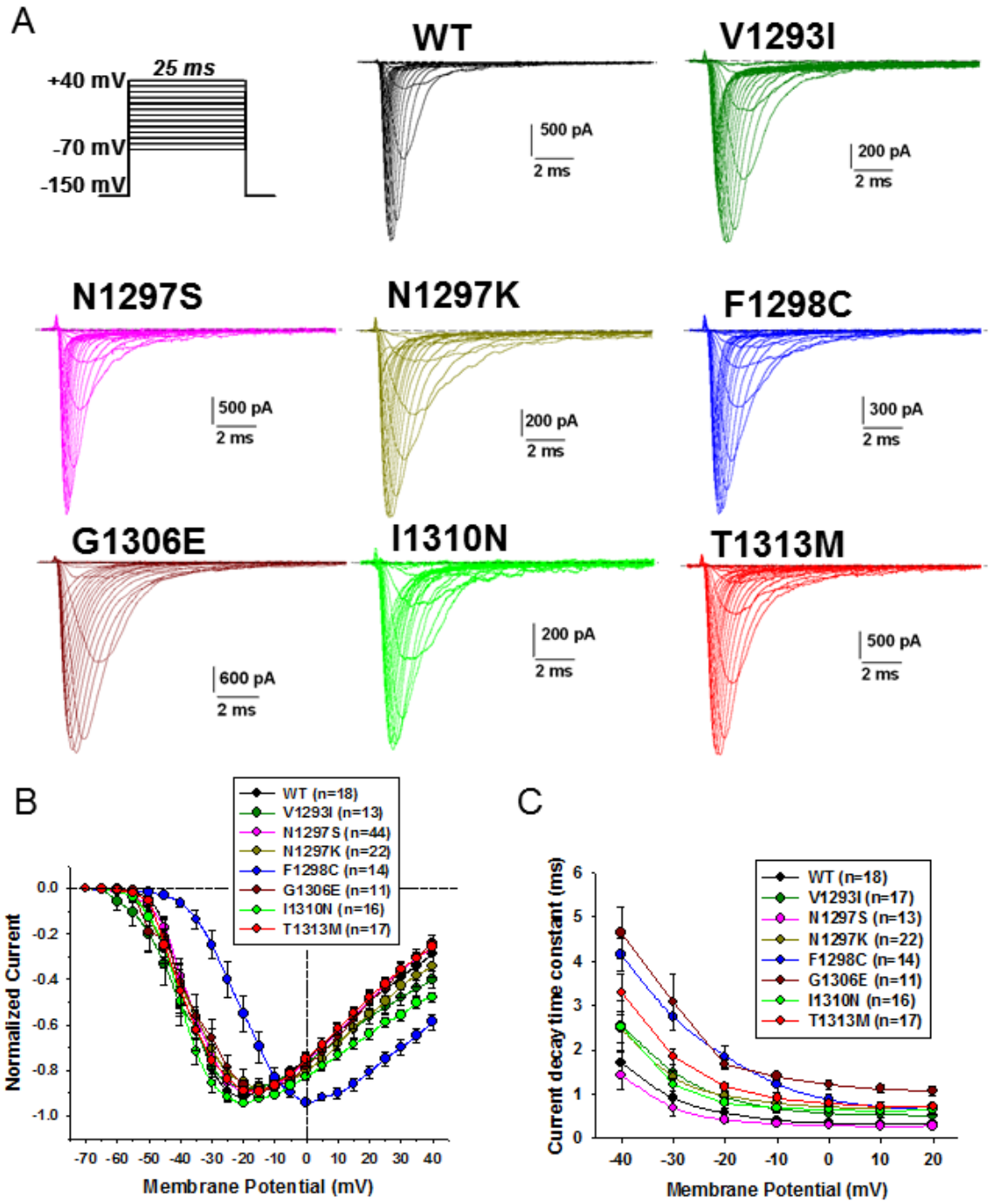

1

Fig. 2 (Farinato et al., 2018)

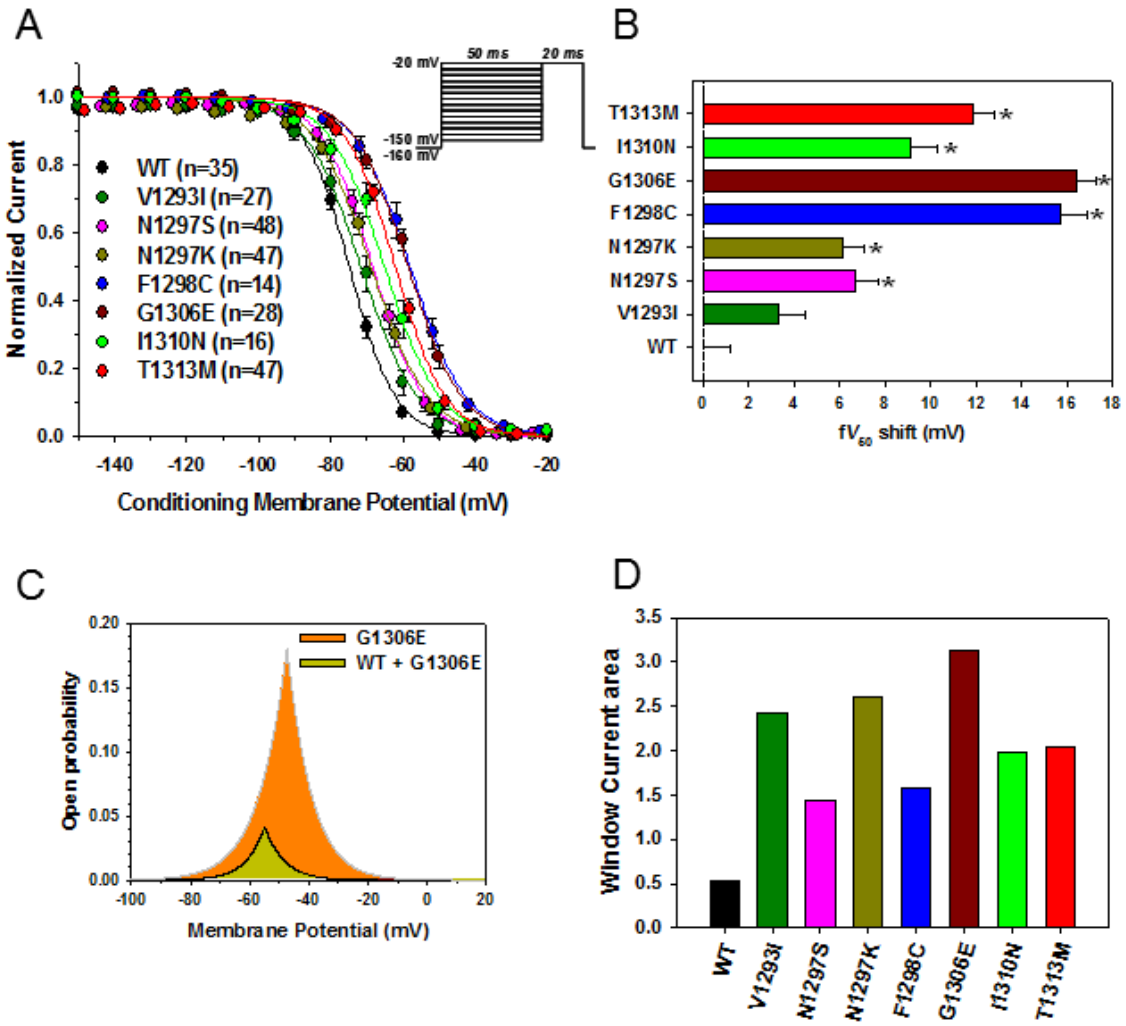

1

Fig. 3 (Farinato et al., 2018)

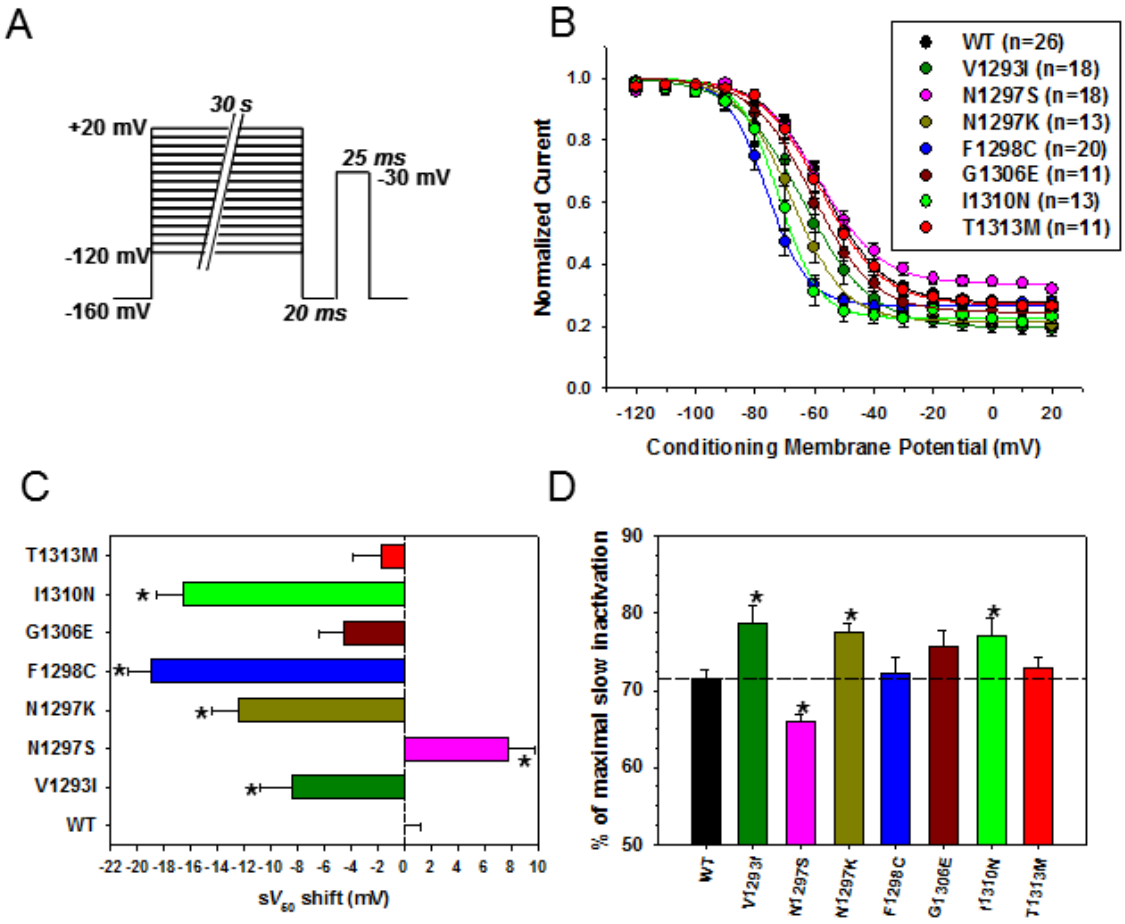

1

Fig. 4 (Farinato et al., 2018)

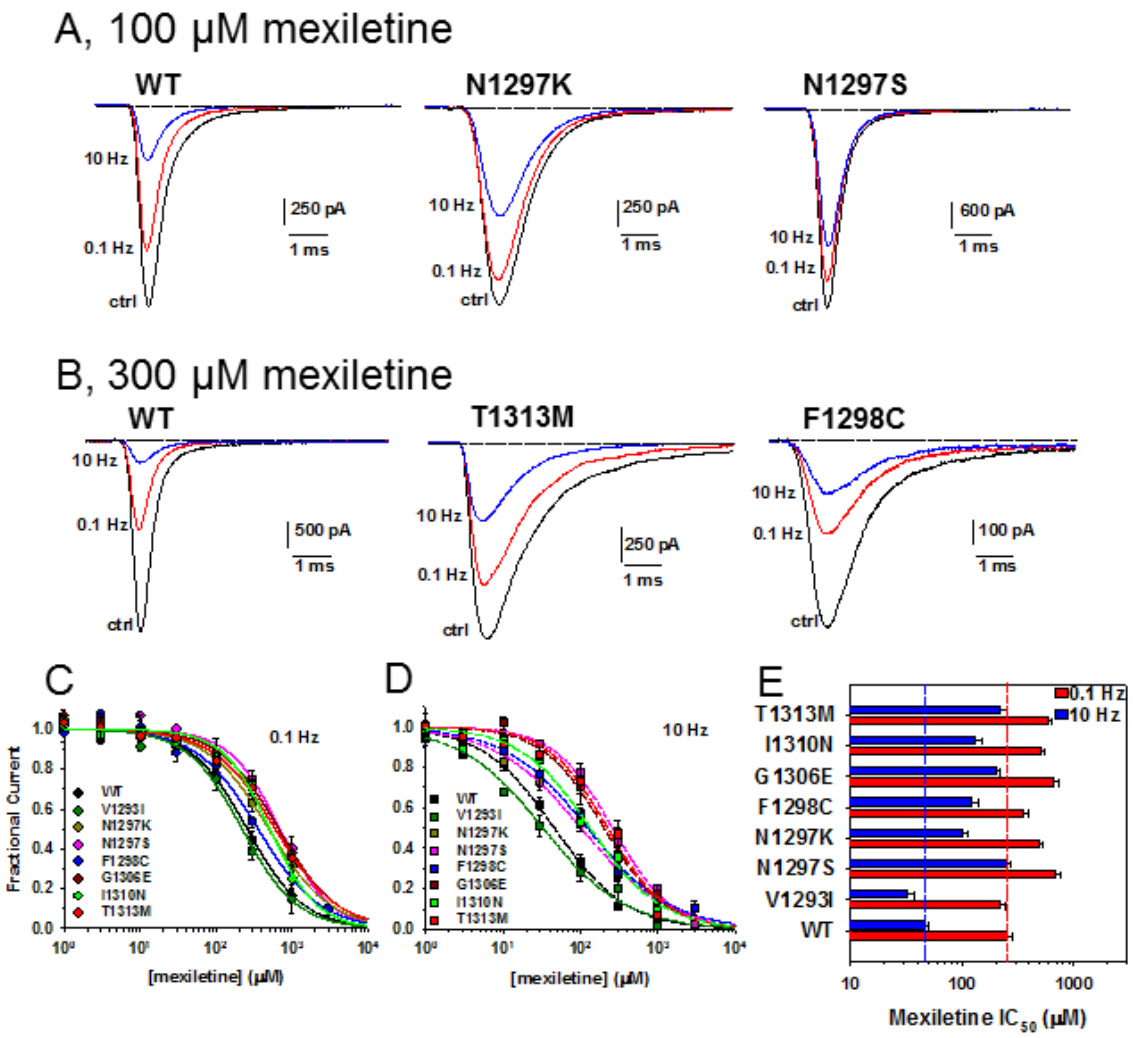

1

Fig. 5 (Farinato et al., 2018)

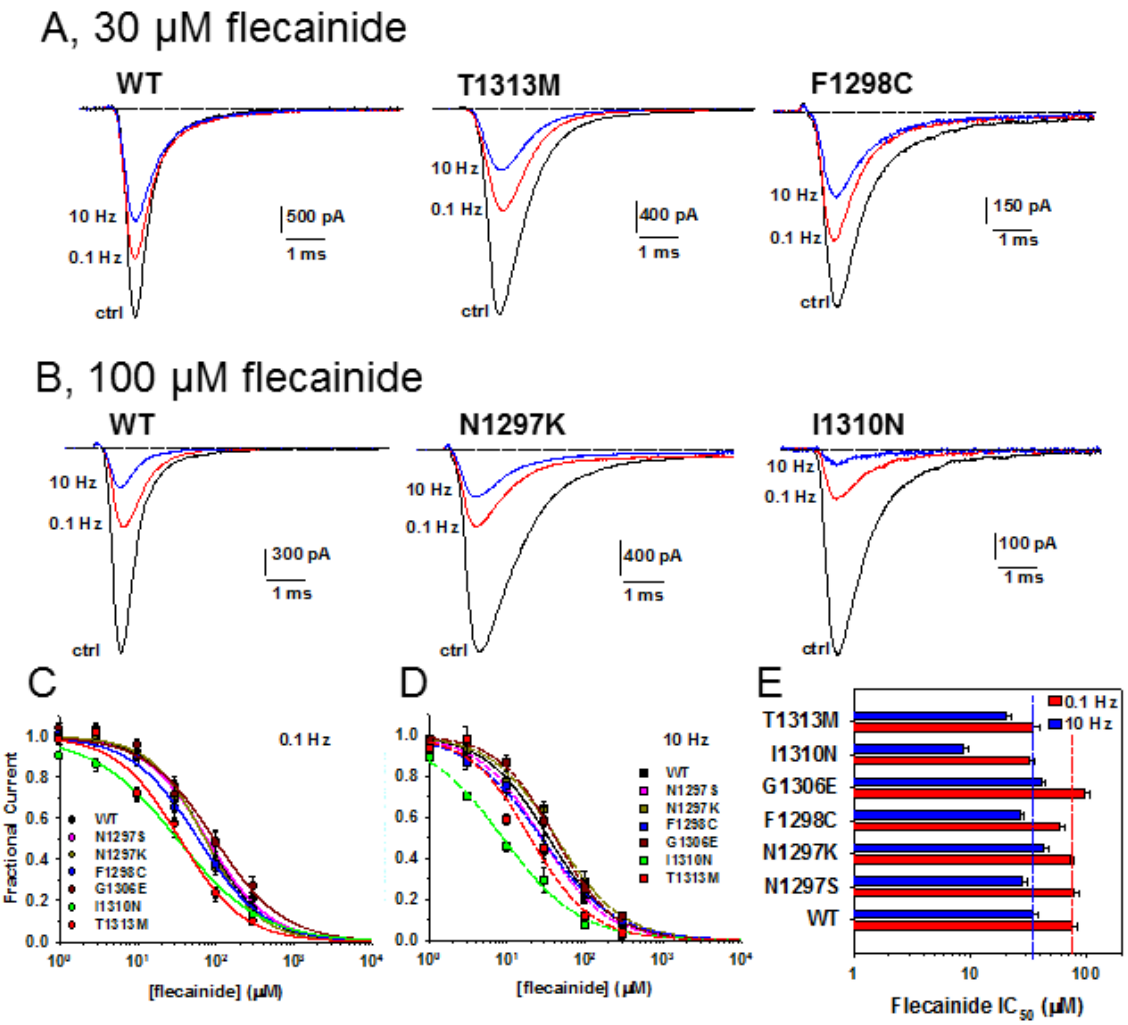

1

Fig. 6 (Farinato et al., 2018)

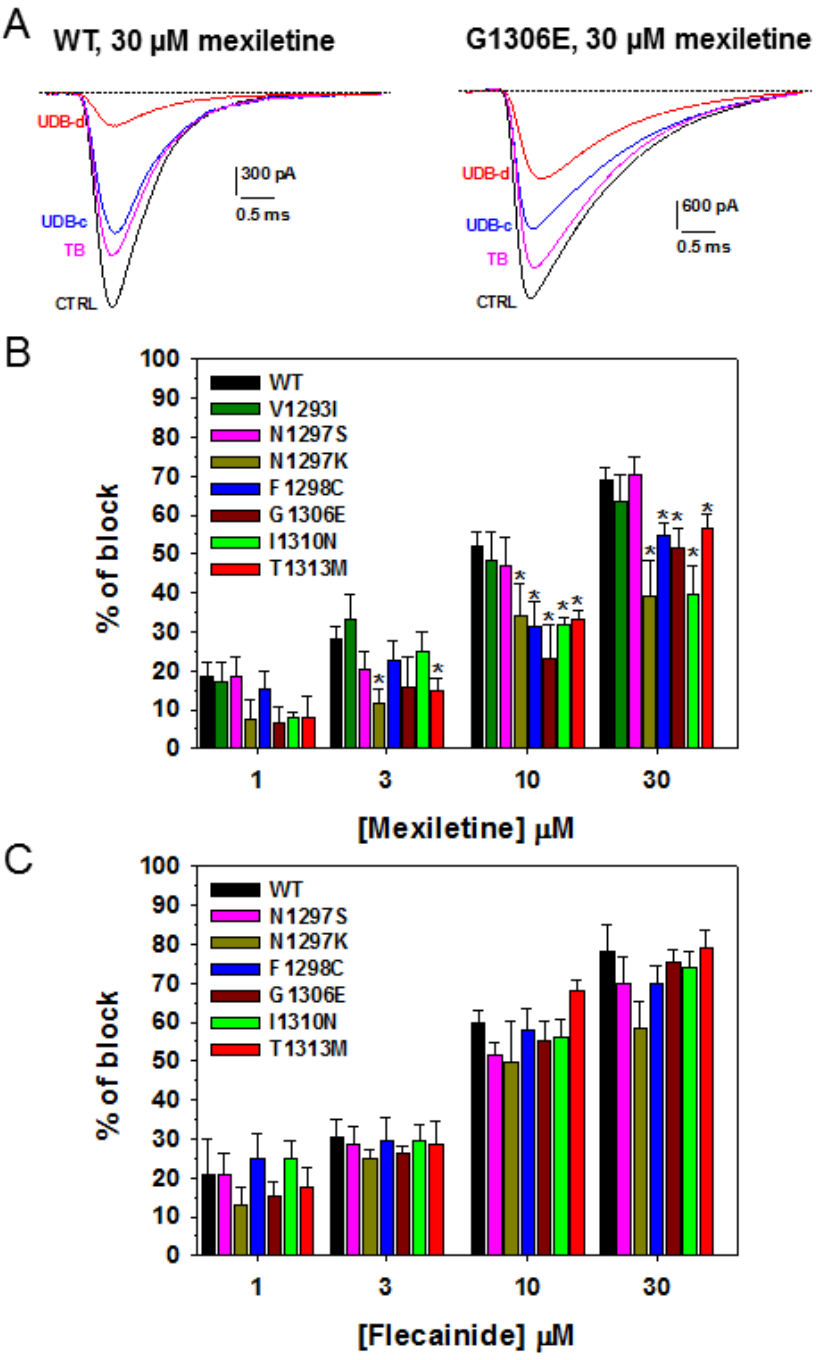

1